

Review

# Progress on the Microcavity Lasers Based on Microstructured Optical Fiber

Yansong He <sup>1</sup>, Jianfei Liu <sup>1,2</sup>, Mingming Luo <sup>1,2,\*</sup> and Huimin Shi <sup>3</sup> 

<sup>1</sup> School of Electronic and Information Engineering, Hebei University of Technology, Tianjin 300401, China; 202031903001@stu.hebut.edu.cn (Y.H.); jfliu@hebut.edu.cn (J.L.)

<sup>2</sup> Hebei Key Laboratory of Advanced Laser Technology and Equipment, Tianjin 300401, China

<sup>3</sup> Intelligence and Information Engineering College, Tangshan University, Tangshan 063000, China; hmshi@tsc.edu.cn

\* Correspondence: mmluo@hebut.edu.cn

**Abstract:** Microcavity lasers are widely applied in bio-chemical sensing, molecular targeted detection, integrated labeling source, and optofluidic control. Particularly, the microstructured optical-fiber-based laser is expected to be a promising candidate for its high-quality factor, low threshold, high integration, and low energy consumption. Moreover, the latest nano technology improves its lasing performance in spectral range, linewidth, and circling lifetime. Considering the specificity in this paper, the discussion presented herein focuses on several typical cases of the microcavity lasers integrated in microstructured optical fiber over the past decades. These micro- and nano-scaled lasers are expected to become a priority in next-generation integrated optics and biomedical photonics.

**Keywords:** microcavity laser; microstructured optical fiber; integrated fiber resonator



**Citation:** He, Y.; Liu, J.; Luo, M.; Shi, H. Progress on the Microcavity Lasers Based on Microstructured Optical Fiber. *Electronics* **2023**, *12*, 1761. <https://doi.org/10.3390/electronics12081761>

Academic Editors: Chengkun Yang, Zhengyong Liu, Rui Min and Yang Yue

Received: 9 March 2023

Revised: 26 March 2023

Accepted: 31 March 2023

Published: 7 April 2023



**Copyright:** © 2023 by the authors. Licensee MDPI, Basel, Switzerland. This article is an open access article distributed under the terms and conditions of the Creative Commons Attribution (CC BY) license (<https://creativecommons.org/licenses/by/4.0/>).

## 1. Introduction

A microcavity laser is defined as a highly integrated laser with different types of resonators, whose geometry is limited to microns or nanometers, at least in one dimension [1]. Exciton behavior and light–matter interaction are proved to be interesting and fertile fields in such micro–nano-scaled cavities [2]. The particle nature of light becomes more significant in microcavity lasers, including high efficiency energy transferring [3], long circling lifetime [4], and low threshold in a high quality-factor (Q) cavity at wavelength or sub-wavelength [4]. Their outstanding performances show applications in optical communications, integrated optics, and nonlinear optics [5].

Theoretically, the ideal microcavity lasers are considered to be non-threshold due to the Pucell confinement in an extremely small scale [6]. In fact, however, their thresholds are supposed to be as low as  $nw/n$  due to the circling loss in an imperfect cavity [7]. The self-absorption also affects the stimulated radiation and energy transferring at molecule level in gain medium, which causes lasing threshold incrementation as well. Thus, a uniform cavity with a high Q and a high efficiency gain medium are the keys to high-performance lasing sources [8].

With the high-precision silica base processing techniques, including femtosecond manufacturing [9], photo-induction etching [10], photonics crystal [11], and the arc modification [12], the micro- and nanocavities become available by means of secondary modifications and are flexible for the longitudinal mode selection. Thus, the exciton electronic transitions couple with stabilized cavity resonant modes when photons are excited in microcavities [13]. Light is easy to oscillate and keep confined in high-quality resonators, including photonic crystal structure [14–16], Fabry–Perot (F-P) microcavity [17–21], and whispering-gallery-mode (WGM) resonators [22,23]. Reflections between optical mirror pairs [24], circling beams in whispering-gallery cavities [25], and light transferring from

the organic materials to adjacent waveguides can all be considered as coupling between excitonic photons and cavity modes [26].

Periodic structures in the photonic crystals cause oscillating lasing at an appropriate wavelength depending on its period size, as shown in Figure 1a [16]. By adjusting the periodic arrangement in the photonic crystal, the lasing wavelength can be flexibly and continuously regulated. Referring to the typical linear cavity in the laser, the Fabry–Perot cavity is achieved with a pair of high-finesse mirrors, as in Figure 1b [19]. The photons generate from the gain medium, start to oscillate between the two planar parallel mirrors, and multiply in the linear cavity. After reciprocating reflection along the central axis, the energy accumulates, exceeds the threshold, and then lases throughout the exiting port. Though the linear cavity can be compressed to a very small scale, these two planar parallel mirrors are extremely difficult to align with each other, leading to a large loss and a low Q. As the laser size can be further compressed along the perimeter of a ring or ring-like cavity, the standing wave satisfying the resonant conditions are defined as whispering-gallery mode (WGM) in Figure 1c [23].

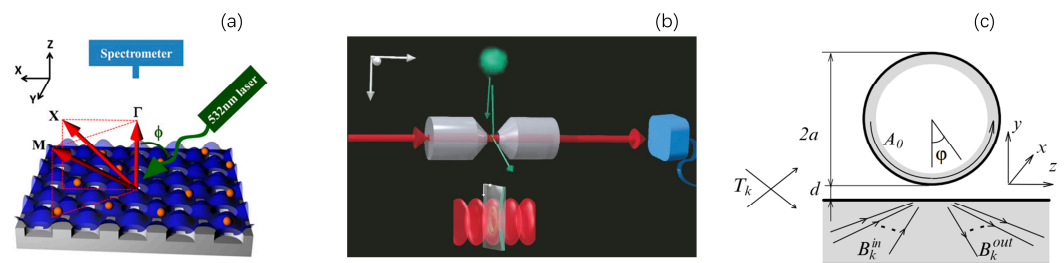


**Figure 1.** Structural diagrams of the typical optical microcavities: (a) Photonic crystal microcavity [16]; (b) F-P microcavity [19]; and (c) Whispering-gallery mode in the form of microspheres [23].

The whispering-gallery mode (WGM) in optics is defined as a resonant ring mode around a ring or ring-like cavity, where the standing waves form at specific wavelengths satisfying the resonant conditions [27].

$$L_c n_{eff} = m\lambda \quad (1)$$

$L_c$  refers to the perimeter of a ring resonator as the cavity length, and  $n_{eff}$  indicates the effective refractive index of the WGMs at specific lasing wavelength  $\lambda$ . Here,  $m$  is an integer relating to the spacing among longitude modes. Considering the refractive index gradient between the cavity and the air, the light would be well confined at the interface by the total internal reflection. The WGMs exist in most of the ring-like cavities, including the droplet, capillary, micro-pillar, micro-ring, and micro-disk, as shown in Figure 2 [28–32].

The lasing performances depend on the shapes, sizes, and materials of the microcavity, predicting the high built-in intensity, low threshold, and narrow linewidth. However, the homemade cavities are not consistent with each other for mass production without standardized manufacturing [33]. An extremely high precision is also required for spatial alignment and low-cost coupling, due to the complex structures in the resonators. Moreover, those highly integrated devices are fragile and vulnerable to temperature, stress, and vibration in practice.

An erbium-doped microcavity laser on a chip is proposed and demonstrated by Yang et al. [34] The high Q resonator is achieved by multi-processing chemical etching and arc modification upon a silicon wafer. The sol–gel films are applied to the silica toroid with erbium-doping as the gain medium, realizing a single longitudinal mode lasing at the  $nJ$  threshold.

Yue Wang et al. proposed a liquid laser emitting blue light at approximately 440 nm, with an exceptionally low threshold and capable of producing quasi-continuous output. Engineering of unconventional ternary QDs with CdZnS/ZnS-alloyed core/shell architecture

was conducted. They leveraged the latest advancements in novel media gain techniques to minimize defects and eliminate Auger recombination [35].

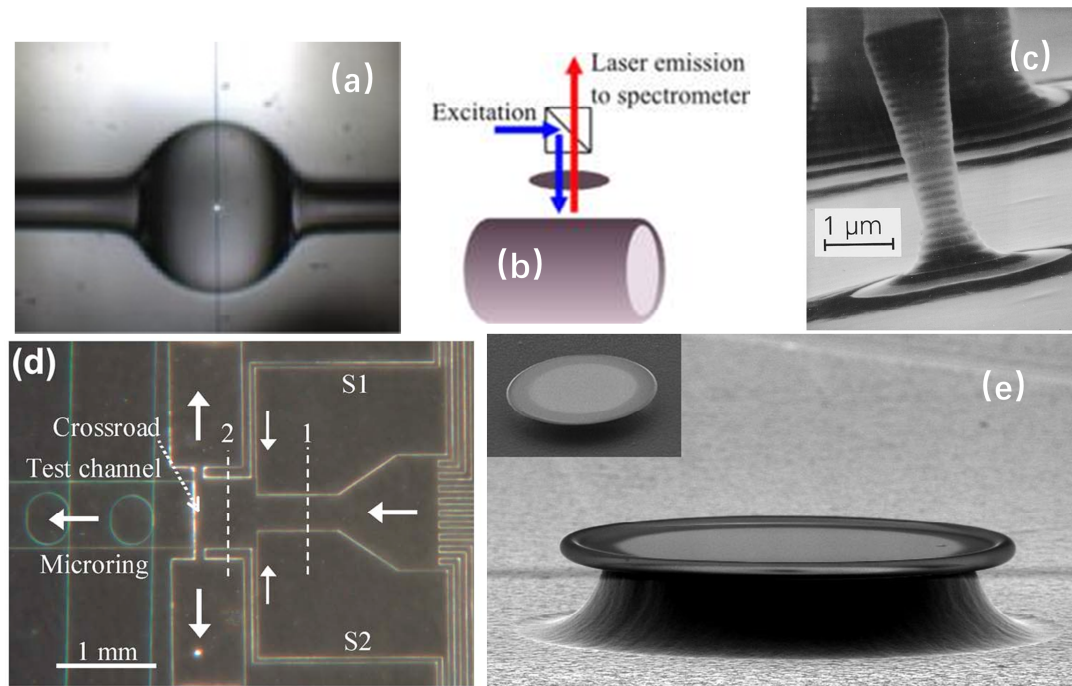


**Figure 2.** Several forms of whispering-gallery microcavities: (a) droplet type [28]; (b) capillary type [29]; (c) microcolumn type [30]; (d) micro-ring type [31]; and (e) micro-disk type [32].

Due to the intricate production process, lack of uniformity, and difficulty in integration, the widespread use of microcavity lasers is restricted. On the other hand, the microstructured optical fiber (MOF) is expected to be a viable platform for micro–nano integration, making it suitable for mass applications.

## 2. Resonant Cavity in Fiber Microcavity Lasers

The integrated microstructures in microstructured optical fibers provide plenty of cavities and subwavelength waveguides with strong evanescent fields, energy confinements, and good uniformity [36]. Furthermore, the built-in penetrating microfluidic channels enable integration with active gain materials [37–41]. Owing to their excellent performances, these fibers are widely used in the manufacture of micro–nano-photonic devices.

### 2.1. Fiber Microcavity Laser Based on Hollow Core Bragg Fiber

Light is localized in hollow Bragg fiber with a two-dimensional Bragg reflector in the fiber cladding due to the photonic band gap guidance. Multilayer dielectric structures in the fiber cladding act as high reflection mirrors, which allow lossless axial transmission at specific wavelengths. In addition, the hollow core provides a high-quality microcavity and a fine optofluidic channel for gain medium integration.

A novel polymer surface-emitting fiber microcavity laser based on hollow Bragg fiber was proposed and demonstrated by Ofer Shapira et al. from Massachusetts Institute of Technology. This laser was capable of long-distance transmission and radial laser emission, with potential applications in laser textiles, as shown in Figure 3. They presented the experimental realization of unprecedentedly thin layer thicknesses of 29.5 nm, which were maintained throughout meter-long fibers, and even achieved lasing at nine different wavelengths with a threshold as low as 89 nJ. This fiber microcavity laser is radially directed from its circumferential surface which paves the way for laser textile fabrics and 3D laser-emitting structures [42].

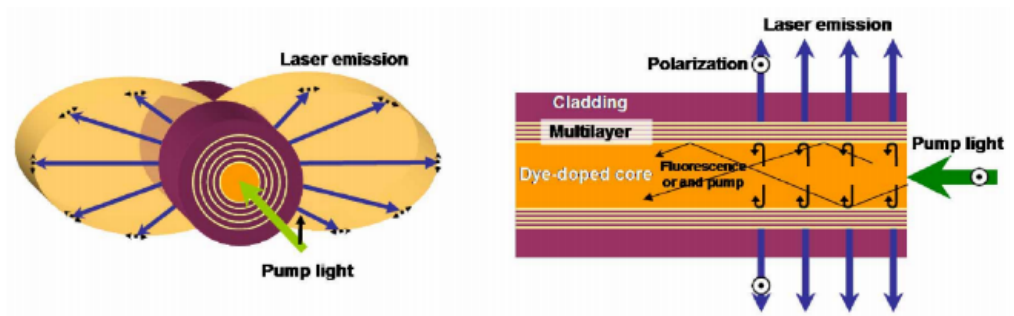


**Figure 3.** Schematic diagram of microcavity laser based on hollow core Bragg fiber, with dye-doped core, axial pump light, and transverse emitting [42].

As shown in Figure 4, Alexander Stolyarov et al. proposed a mirror-emitted zero-angular momentum microcavity laser using hollow Bragg fibers in 2012. The microcavity laser was axially pumped to achieve an electrically contacting and independently addressable liquid crystal microchannel array in a single fiber [43]. It is of far-reaching significance to develop a new type of fiber microcavity laser that has low cost and good repeatability, and is easy to realize; however, the axial pumping method still needs improvement in coupling efficiency.

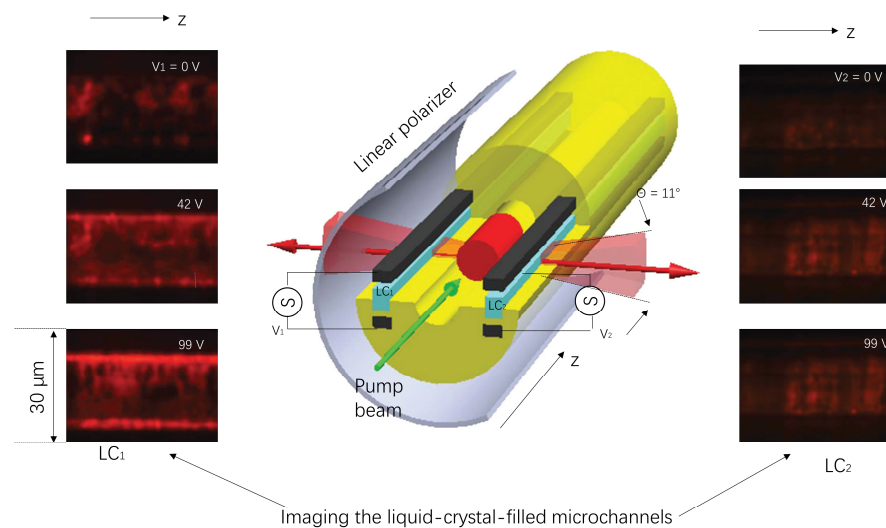


**Figure 4.** Schematic of zero-angle momentum microcavity lasers based on hollow Bragg optical fibers [43].

Moreover, although no additional microfluidic channels are required in the hollow core Bragg fiber based lasers, which simplifies the secondary fiber processing and experimental setup, the optofluidic lasing can be achieved only by axial pumping because of the optical feedback realized in the intrinsic structure of the fiber. The periodic micro/nanopillars on top of a planar waveguide act as both the Bragg grating and superhydrophobic surface, which promises a narrow bandwidth of 0.4 nm and a wide wavelength tuning range greater than 25 nm [44]. Thereafter, J. Hu et al. presented the lasing performances of a three-layer Bragg fiber resonator, consisting of a dye-doped cholesteric liquid crystal (DDCLC) microdroplet, polyglycerol-2, and a hollow glass microsphere in 2019 [45].

2.2. Fiber Microcavity Laser Based on Fabry–Perot Cavity

The Fabry–Perot resonator is a typical optical feedback structure used in optical fiber microcavity lasers. Considering its high temperature resistance, miniaturization, and manufacture, the Fabry–Perot resonator is suitable for harsh conditions and small-scaled space.

In 2003, Kristense et al. developed an optical microfluidic dye laser [46]. Using the ethanol solution of rhodamine 6G as the laser gain medium and the second harmonic Nd:YAG laser as the pump source, the laser resonance was successfully realized in the F-P cavity composed of metal mirrors, which opened the door for the F-P cavity fiber microcavity laser. In 2006, Q. Kou of the University of Paris 11 in France presented a device consisting of two parallel metal mirrors to form a F-P laser resonator, which were coated on the end face of the optical fiber and integrated into a polydimethylsiloxane chip. Then, an on-chip collinear two-color microfluidic dye laser, as shown in Figure 5a, was fabricated using rhodamine 6G and sulforhodamine as the gain media [47].

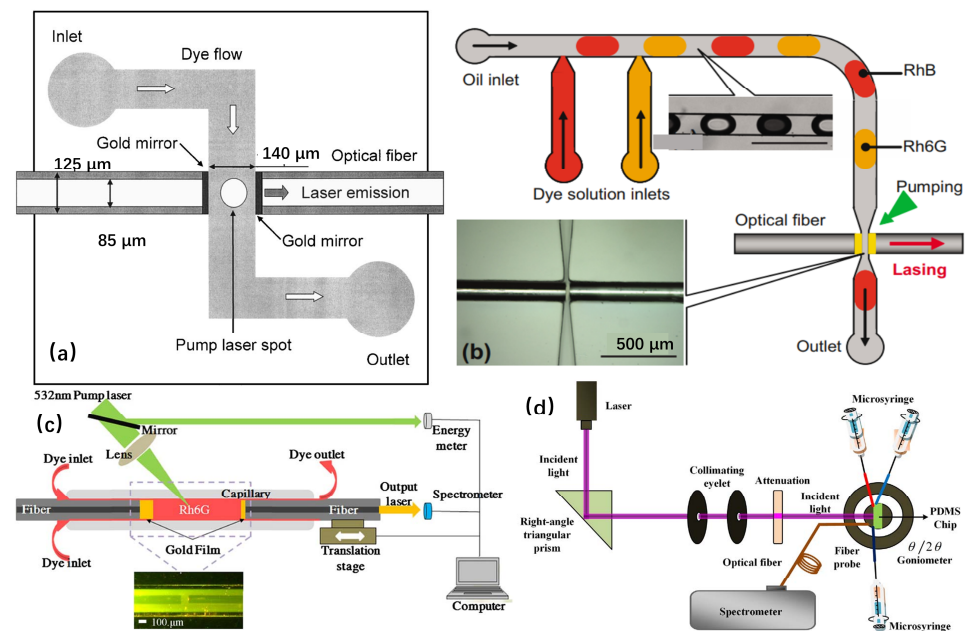


**Figure 5.** Schematic diagram of a microcavity laser based on an F-P cavity. (a) On-chip co-linear two-color microfluidic dye laser [47]; (b) Fast-switching microcavity laser with two different dye droplet streams [48]; (c) Laser wavelength tunable microcavity laser [49,50]; and (d) White dye laser [51].

In 2011, based on the research results of Q. Kou, the G. Aubry team of the University of Paris 11 combined the Fabry–Perot cavity with a fiber mirror to form a microfluidic dye laser, and a single longitudinal mode emitted laser was obtained by rapidly switching the droplet flow of two different dyes, as seen in Figure 5b [48]. In 2013, H. Zhou et al. of Sichuan University realized the laser wavelength tunability of wide 18nm and the integration of an on-chip laboratory system by controlling the cavity length by forming a F-P cavity consisting of quartz capillaries and two gold-plated aligned fibers, as in Figure 5c [49]. In 2015, R. M. Gerosa of McKinsey Church University in Brazil realized high repetition rate optical fluidic laser output of all-fiber structure based on Fresnel reflection of optical fiber end face [50]. In 2018, the Y. Kong research group of Shanghai Jiaotong University realized the low threshold white dye laser emission through laminar flow control using the F-P cavity formed by coated fibers at both ends, demonstrating the simultaneous multi-wavelength fiber microcavity laser on the integrated system, as shown in Figure 5d [51]. Bin Zhang presented an experimentally demonstrated 3D-printed castle-style F-P microcavity on an optical fiber tip for humidity sensing in 2019. Repeated experiments have demonstrated that the 3D-printed castle-style F-P microcavity humidity sensors are repeatable and stable. Such sensors show excellent sensing performance with a compact structure, high sensitivity, fast response, and good stability, making them highly promising for humidity sensing applications [52].

To sum up, as a simple optical cavity, the F-P resonator can make the operating material oscillate in the cavity all the time and reduce the loss to the minimum, so it can be used in high-power pulsed lasers [53]. However, in the actual operation, the F-P resonator requires high precision, which is difficult to achieve, and it is difficult to meet the requirements of the quality factor, so the application field is not very wide. In order to realize the luminescence and heating of this type of microcavity laser in sensing and biological detection, it is necessary to simplify the laser construction form further, reduce the cost, or improve the Q value of F-P cavity in a better way.

### 2.3. Fiber Microcavity Laser Based on Fiber Micro-Ring Resonator

The micro-ring resonator is a resonant cavity based on the echo wall mode (whispering-gallery mode, WGM). The light is bound in the resonant cavity and propagates in the way of approximate total internal reflection. In this process, the light is excited and amplified. The traditional echo wall mode microcavity is often used in semiconductor microcavity lasers. For example, in 2010, the research group of Professor Yang Lan of Washington University in St. Louis proposed a microcavity laser with an ultra-high-quality factor echo wall mode resonator based on WGM and used it for the quantitative detection of single nanoparticles, which can not only simplify the process of nanoparticles detection but also achieve high resolution quantification [54]. However, with the development of optical fiber technology, the fiber laser based on the fiber micro-ring resonator has been favored by researchers at home and abroad because of its good stability and low cost. Therefore, it has become the focus of the current research to optimize the performance of this type of microcavity laser in different ways. In the past decade, researchers have effectively improved the performance parameters of microcavity lasers by using different optical fibers to make optical resonators. In 2009, Sun of the University of Missouri in the United States developed a dye laser based on OFRR (optical microfluidic ring resonator) using communication fiber combined with capillaries and achieved a threshold of  $7 \text{ nJ/mm}^2$  laser output per pulse, as shown in Figure 6 [55,56].

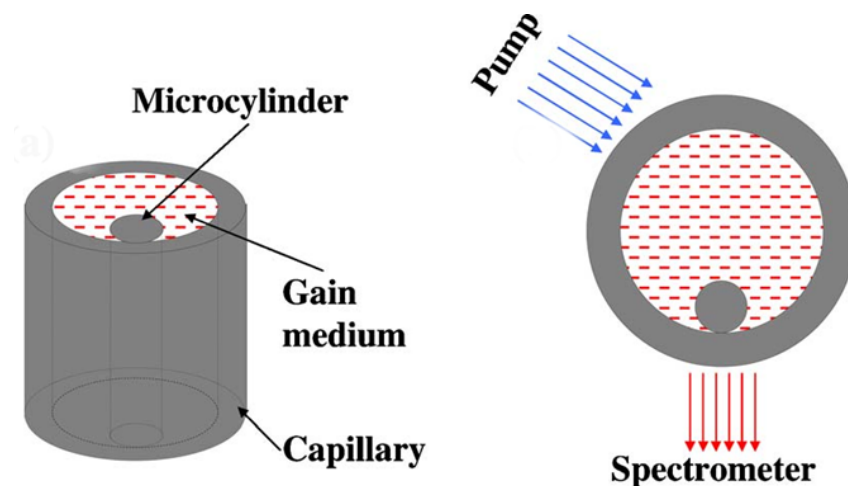


**Figure 6.** Side view and section view of communication fiber dye laser [55,56].

In 2013, Z. Li of Nankai University and others developed a microcavity laser using a simplified hollow microstructure fiber with a submicron thickness ring resonator. The special structure of this type of optical fiber can be regarded as the combination of silica micro-ring and microfluidic channel so that the structure becomes more compact. In the follow-up research, a low-threshold laser was realized after filling the central air hole with organic dyes, and a compact, efficient, and stable optical flow microcavity laser [57] was proposed. In 2015, Z. Li et al. obtained wavelength tunable laser excitation by controlling the liquid surface position of the filling material in the tapered simplified hollow microstructure fiber (Figure 7) [58].

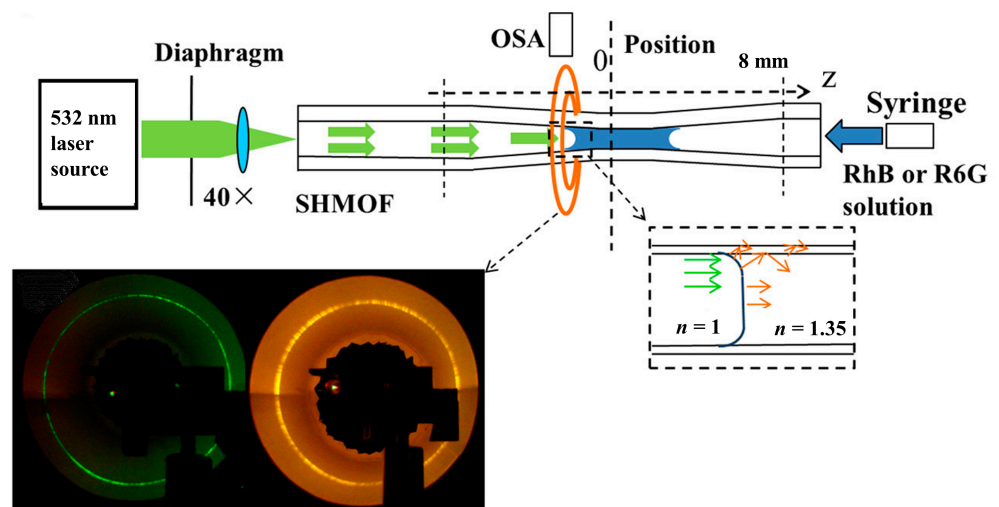


Figure 7. Schematic diagram of simplified hollow microstructure fiber microcavity laser [58].

In 2017, Gong et al. reported a low-cost, repeatable fiber-optic microfluidic laser using double-hole microstructure fiber and carried out experimental observation and numerical simulation analysis on the angle dependence of laser emission, which has a great prospect in reducing the cost of biological monitoring [59]. In 2018, Gao et al. combined femtosecond laser technology with hollow optical fiber to prepare an air hole in the cladding of optical fiber to realize the detection of highly toxic polycyclic aromatic hydrocarbons. Because of the immune reaction between the antibody and the target B [a] P, the B [a] P molecule can be detected by anti-resonance reflection optical waveguide (Figure 8) [60].

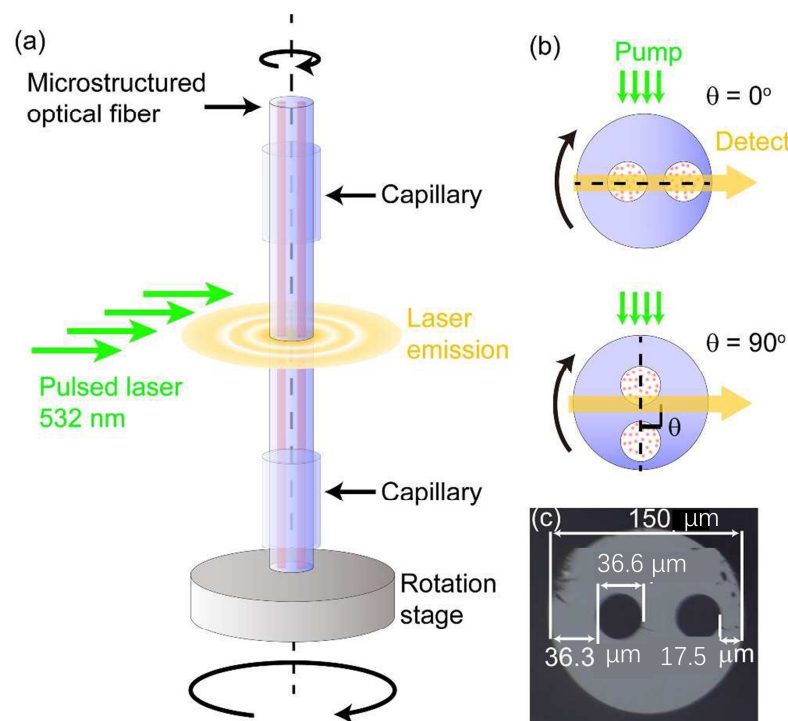


Figure 8. Dual-hole microstructure fiber-based microcavity laser. (a) Schematic diagram of the experimental setup; (b) Schematic cross-sectional view; and (c) Cross-sectional electron microscope image [59].

In the same year, Jie Yu et al. developed an optical microfluidic laser with a threshold as low as  $14 \text{ nJ}/\text{mm}^2$  using hollow negative curvature anti-resonant fiber. The laser had a com-

pact structure and was able to realize directional emission [61]. Zhang, M., et al. proposed a tunable optical Bragg grating filter based on the surface drop effect of superhydrophobic nanopillar arrays. The results showed that this approach has great potential for designing and fabricating tunable optical microcavity with high precision and stability. The study provided new insights into the development of advanced microcavity lasers and has important implications for various applications, from optical communication to sensing and imaging [62]. In 2019, Y. Xu et al. realized a repeatable optical microfluidic microcavity laser for multi-channel biochemical sensing using a hollow fiber. This type of laser has good repeatability, is easy to integrate, and has a good prospect in the field of biochemical detection [63]. In 2020, J. Lin et al. used cholesteric liquid-crystal-doped laser dyes to infiltrate the microstructure fiber and realized the all-optical emission direction control of microcavity lasers with low threshold and large circularly polarized anisotropy, which provided a new solution for phototherapy, display, sensor, and so on [64].

Overall, the difficulties of using communication fiber to realize fiber microcavity laser lies in the fabrication of micro-ring resonator. With its unique structure (such as having natural laser gain medium channel), various microstructure fibers have unique advantages in improving fiber microfluidic microcavity lasers. The selection of various microstructure fibers can allow for laser miniaturization, integration, reduced cost, and improved repeatability.

### 3. Gain Medium in Fiber Microcavity Lasers

Materials in different forms, states, and combinations have been demonstrated in microcavity lasers, and their energy levels enable emissions at different wavelengths from ultraviolet (UV) to infrared. Organic dyes, quantum dots (QDs), fluorescent bioprotein, and rare earth elements have been tested and optimized to achieve higher optical gain and better lasing performances.

#### 3.1. Organic Dyes

As a laser gain material, organic dyes have many advantages, such as controllable laser wavelength, high fluorescence efficiency, low laser threshold, low cost, and so on. However, at the same time, the easy bleaching of organic dyes seriously affects the stability of laser emission. Organic dyes have been widely used as gain materials for liquid lasers due to their high quantum yield, brightness, broad spectrum coverage, low threshold, and low cost. However, photobleaching of organic dye can reduce the stability of laser output. To reduce this adverse effect, a continuous flow of dye solution or a decrease in the repetition rate of the pump laser, even a single-pulse pump, can be employed.

Moon, H. J., et al. demonstrated that a cylindrical microcavity of 125  $\mu\text{m}$  diameter was filled with rhodamine 6G dye molecules in an ethanol solution of lower refractive index, enabling the whispering-gallery modes of the microcavity to be stimulated by a second harmonic of a Nd:YAG laser, resulting in laser oscillation in the evanescent field region outside the cavity [65]. Hao Zhou presented a tunable fluidic dye laser formed by a microcavity filled with a rhodamine 6G dye solution. By controlling the cavity length, we are able to achieve a wide 18 nm tunability of the laser wavelength. The microcavity is composed of a silica capillary and two aligned fibers with Au-coated end faces. The dye solution is pumped by 532 nm wavelength laser pulses, resulting in laser emission of approximately 570 nm in the form of TE mode with a threshold of approximately 58  $\mu\text{J}/\text{pulse}$  [49].

In 2014, Z. Li of Nankai University and others fabricated optical fluidic microcavity lasers using simplified hollow microstructure fibers filled with different concentrations of rhodamine dye and proposed a lateral high efficiency fluorescence detection technique based on charge coupling, which increased the detectable concentration limit by two orders of magnitude [66]. Figure 9 presents the schematic diagram of organic dye gain microcavity laser.

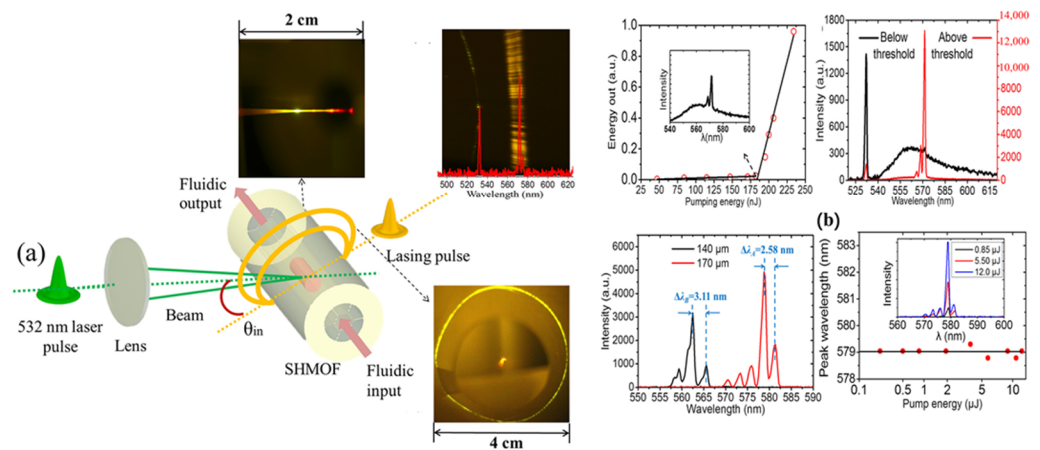


**Figure 9.** Schematic Diagram of Organic Dye Gain Microcavity Laser. (a) Layout of laser experimental system and (b) Output laser spectrum and resolution spectrum [66].

In 2018, Chaoyang Gong et al. presented a fiber optofluidic laser (DFOFL) and demonstrated its potential for high-throughput sensing applications. Additionally, the DFOFL wavelength can be fine-tuned over hundreds of nanometers by altering the dye concentration or reconfiguring the liquid gain materials [67]. In 2018, D. Yan et al. realized dye laser embedded in Kagome photonic crystal fiber with methanol and high refractive index dye solution as a gain medium, which had good robustness and compactness [68].

In addition, lasing can also be achieved by solidifying dyes in a film; the dye-doped polymer or the conducting polymer itself can be applied as a thin film on the inner surface of HOF or on the outer surface of telecom optical fiber to demonstrate lasing [69–71].

X. Zhao et al. presented a hollow optical fiber optofluidic laser utilizing a dye-doped polymer film. In this study, they reported on the laser spectra and threshold properties of the HOF micro-laser. The dye-doped polymer film can be adjusted to a thickness of 1.6  $\mu$ m, achieving a threshold of less than 1  $\mu$ J/mm<sup>2</sup> [69].

### 3.2. Biological Gain Materials

The biofluorescence is often found in marine creatures and insects, where enzyme protein releases energy in metabolic process. Thus, the macromolecular protein or DNA can be utilized as fluorescent labels in biochemical tests. Due to their good compatibility and affinity, the biochemical gain materials can be implanted in cells or tissues without toxic side effects.

Y. Sun and X. Fan et al. proposed an optical microfluidic microcavity laser using DNA samples and probes as laser gain media. Compared with the traditional fluorescence detection methods, the resolution of this laser system was improved by two orders of magnitude, which provided the possibility for the highly specific detection of DNA molecules [72].

Q. Chen's team used fluorescent protein, dye-labeled bovine serum albumin, and DNA samples as gain media to realize an optical microfluidic laser based on the echo wall mode resonator [73].

Wonsuk Lee et al. realized the optical microfluidic laser emission of monolayer gain by using DNA molecules as gain materials. This laser detection method greatly improved the detection efficiency, simplified the detection process, and reduced the consumption of tested samples; the optical setup utilized in the experiment is illustrated in Figure 10 [74].

The lasing mechanism of these biomaterials is analogous to that of a quasi-four-level laser system. The short lifetime of biological gain materials in the excited state allows for population inversion to be achieved most efficiently through optical pumping with nanosecond or shorter pulses [75].

Through the study of the above literature, we know that biomaterials, such as fluorescent proteins, can be used in the biological detection of microcavity lasers due to their good biocompatibility, non-pollution, and low cost; however, in the excited state, the life of

biomaterials is very short, and there is no way to solve it at present, so it is used mainly in the laboratory stage.

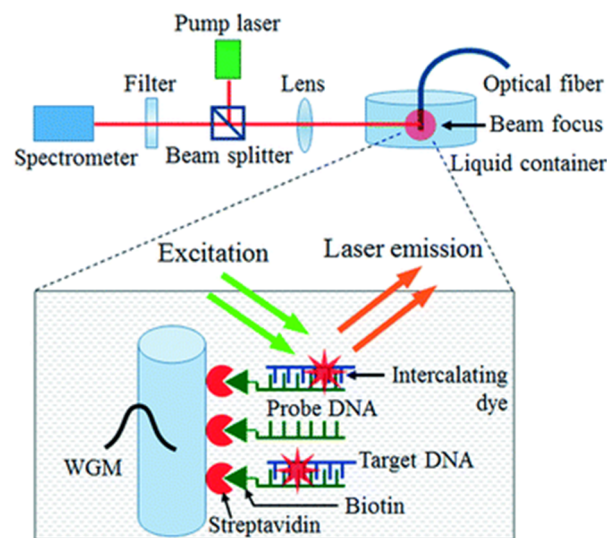


**Figure 10.** Fiber OFRR in liquid environment is confocally pumped with an OPO laser source, where the evanescent field of the guided WGM interacts with surface-attached molecules and provides feedback for lasing phenomena [74].

### 3.3. Quantum Dot

Quantum dot lasers are semiconductor lasers that use quantum dots as the gain medium. Quantum dots are nanometer-sized semiconductor particles that can be engineered to emit light at specific wavelengths. Quantum dot lasers offer several advantages over traditional semiconductor lasers, including higher efficiency, better beam quality, and the ability to tune the emission wavelength. They are used in a variety of applications, including optical communications, sensing, and medical imaging [75–77].

This requires researchers to find various ways to eliminate the effects of photobleaching. In addition, when organic dyes are used in biological detection, it is easy to cause damage to the detected biological samples, which also restricts the development of this type of laser. Different from organic dyes, quantum dots (QDs) have high optical stability and wide absorption spectrum range (which can avoid the overlap of excitation spectrum and emission spectrum). The fiber microcavity laser based on quantum dots can bring stable and color-adjustable low-threshold laser output, so it has good application prospects in laser gain medium. The microcavity laser made of quantum dots as the gain medium can effectively improve the stability and anti-interference performance of the optical microfluidic laser and greatly reduce the laser threshold of stimulated radiation. In addition, the chemically modified quantum dots have good biocompatibility and can be used for the labeling and detection of biological samples, which should be the focus of future research.

Y. Wang et al. realized the WGM microcavity laser using CdZnS/ZnS alloy core-shell quantum dots as the gain medium. This type of laser can emit ultra-low-threshold blue laser, which has higher optical stability than the traditional organic dye microcavity laser [35]. Alper Kiraz of the University of Cossa in Turkey and others used CdSe/ZnS quantum dot solution as the gain medium for photofluid ring resonant microcavity lasers to achieve high-quality factor laser emission, and the laser threshold is more than three orders of magnitude lower than the existing technology in 2015; this proves that the strong stability of quantum dot laser is obviously better than that of organic dyes, which also lays a foundation for the research of quantum dot optical microfluidic lasers. The spectrum of quantum-dot-filled fiber microcavity laser is shown in Figure 11 [29].

In 2016, N. Zhang of Nanyang Technological University and others demonstrated a type of fiber microcavity laser doped with CdSe/CdZnS/ZnS quantum dots in the

hollow cavity of multi-layer photonic bandgap fiber, realizing azimuth polarization radial emission with zero angular momentum, which provides a new idea for the development of omni-directional display [78].

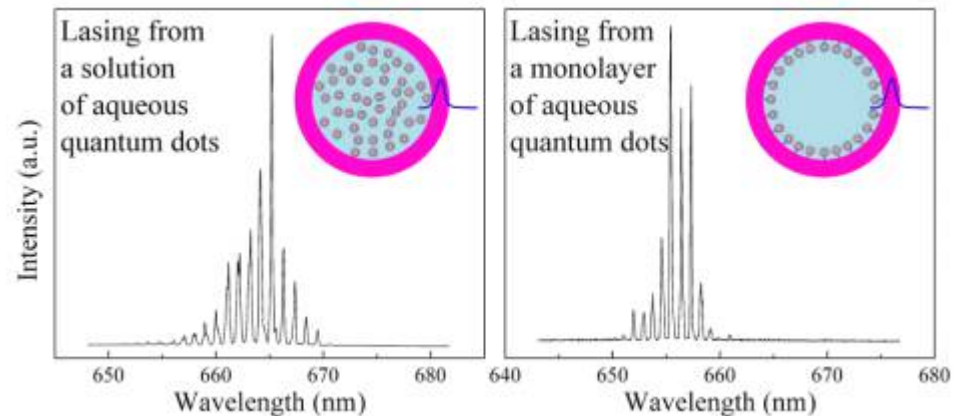


Figure 11. Spectrum of quantum-dot-filled fiber microcavity laser [29].

#### 4. Discussion

In this paper, the latest progress of fiber microcavity lasers is reviewed, including fiber microcavities, gain materials, and pumping. We believe that the innovations in gaining materials and biomaterials, as well as novel designs for fiber optic micro-resonators, will continue to drive fiber optic fluidic microcavity lasers to a better aspect.

Optical fiber microfluidic laser technology has the advantages of high Q value, high sensitivity, ease of integration, low power consumption, and tunability, and has high practical value in environmental monitoring, biochemical sensing, integrated circuits, and other fields. Especially in the field of biological detection, the detection limit of fiber microcavity laser is very low, and it can detect the subtle concentration changes of the tested samples very sensitively, so it has high research value and application prospect. However, most of the current fiber microcavity lasers have various problems, such as poor stability, complex fabrication process, and so on. Many achievements remain in the stage of theoretical research, and further research and experiments are needed. Although researchers all over the world have made great breakthroughs in the field of fiber microcavity lasers, there are still many shortcomings and defects. The quantum dot fiber microcavity laser has high research value because of its excellent stability, but the traditional perovskite quantum dots have some defects that must be solved, such as high cost, complex preparation process, high toxicity, poor water solubility, and so on. In addition, blue-green perovskite is inefficient and unstable, and it decomposes easily, which affects the research and promotion of quantum dot fiber lasers. The novel ZnS quantum dots not only greatly improve the fluorescence properties and quantum yield but also improve the biocompatibility, so it is expected to be used in a wide range of fields. At present, our research group is studying the combination of the echo wall mode optical microcavity with a new quantum dot gain medium, and we are working to strengthen the interaction between pump light and working material in the form of axial pump. It is expected to achieve low threshold quantum dot laser emission with high light intensity and light stability.

Although the microstructured optical fiber is now a conventional and commercial waveguide, its practical use in microcavity laser is still in the stage of proof of principle. Based on the previous research cited above and our own work [59,79,80], lasing performances of the microcavity lasers depend mainly on the microstructures of their cross-section. The geometrics of the subwavelength waveguide embedded in the simplified hollow core fiber, as an example [61], determine distribution of the evanescent field, directly affecting the coupling efficiency and indirectly affecting the lasing threshold. In addition, cavity length of the integrated lasers relies on the perimeter of the ring or ring-like structure, which can be flexibly tuned by a tapered microstructured optical fiber [80]. Moreover, the

effective refractive index of the standing WGMs is not only related to the optical confinement but also determines the specific mode selection, such as directional lasing or single longitudinal mode lasing [81,82]. Thus, microstructures depend a lot on practical use of the integrated microcavity lasers, which can be optimized to improve lasing performances.

**Author Contributions:** J.L. is responsible for literature induction and summary, and H.S. is responsible for literature retrieval and screening. Y.H. is responsible for writing various parts of the review. M.L. is responsible for unifying and integrating the content of the overview. All authors have read and agreed to the published version of the manuscript

**Funding:** This work is supported by the Natural Science Foundation of China (Grant No. 62105092), the Natural Science Foundation of Hebei Province (A2020202013, F2021202054), and the Foundation of Key Laboratory of Opto-Electronics Information Technology of Ministry of Education, Tianjin University (2021KFKT013).

**Data Availability Statement:** The data that support the findings of this study are available from the corresponding author upon reasonable request.

**Conflicts of Interest:** The authors declare no conflict of interest.

## References

1. Vahala, K. Optical microcavities. *Nature* **2003**, *424*, 839. [[CrossRef](#)] [[PubMed](#)]
2. Xiao, Y.; Liu, Y.; Li, B.; Chen, Y.; Li, Y.; Gong, Q. Strongly enhanced light-matter interaction in a hybrid photonic-plasmonic resonator. *Phys. Rev. A* **2012**, *85*, 031805. [[CrossRef](#)]
3. Coles, D.; Somaschi, N.; Michetti, P.; Clark, C.; Lagoudakis, P.; Savvidis, P.; Lidzey, D. Polariton-mediated energy transfer between organic dyes in a strongly coupled optical microcavity. *Nat. Mater.* **2014**, *13*, 712–719. [[CrossRef](#)]
4. Jiang, X.; Xiao, Y.; Zou, C.; He, L.; Dong, C.; Li, B.; Li, Y.; Sun, F.; Yang, L.; Gong, Q. Highly unidirectional emission and ultralow-threshold lasing from on-chip ultrahigh-Q microcavities. *Adv. Mater.* **2012**, *24*, OP260. [[CrossRef](#)]
5. Bravo-Abad, J.; Rodriguez, A.; Bermel, P.; Johnson, S.; Joannopoulos, J.; Soljačić, M. Enhanced nonlinear optics in photonic-crystal microcavities. *Opt. Express* **2007**, *15*, 16161–16176. [[CrossRef](#)] [[PubMed](#)]
6. Spillane, S.; Kippenberg, T.; Vahala, K. Ultralow-threshold Raman laser using a spherical dielectric microcavity. *Nature* **2002**, *415*, 621–623. [[CrossRef](#)]
7. Tang, L.; Yoshie, T. High-Q hybrid 3D-2D slab-3D photonic crystal microcavity. *Opt. Lett.* **2010**, *35*, 3144–3146. [[CrossRef](#)] [[PubMed](#)]
8. Zhou, H.; Yuan, S.; Wang, X.; Xu, T.; Wang, X.; Li, H.; Zheng, W.; Fan, P.; Li, Y.; Sun, L.; et al. Vapor growth and tunable lasing of band gap engineered cesium lead halide perovskite micro/nanorods with triangular cross section. *ACS Nano* **2017**, *11*, 1189–1195. [[CrossRef](#)] [[PubMed](#)]
9. Wang, X.; Yu, H.; Li, P.; Zhang, Y.; Wen, Y.; Qiu, Y.; Liu, Z.; Li, Y.; Liu, L. Femtosecond laser-based processing methods and their applications in optical device manufacturing: A review. *Opt. Laser Technol.* **2021**, *135*, 106687. [[CrossRef](#)]
10. Bakhshkandi, R.; Ghoranneviss, M. The Effect of Heat Treatment on Growth of TiO<sub>2</sub> Nanorods. *J. Nov. Appl. Sci.* **2015**, *4*, 852–856.
11. Knight, J. Photonic crystal fibres. *Nature* **2003**, *424*, 847–851. [[CrossRef](#)] [[PubMed](#)]
12. Berneschi, S.; Barucci, A.; Brenci, M.; Cosi, F.; Farnesi, D.; Conti, G.; Pelli, S.; Soria, S.; Righini, G. Optical Microbubble Resonator: A Novel Structure for Sensing Applications. In *Sensors, Proceedings of the First National Conference on Sensors, Rome, Italy, 15–17 February 2012*; Springer: New York, NY, USA, 2014; pp. 359–362.
13. Chang, H.; Zhang, J. From cavity optomechanics to cavity-less exciton optomechanics: A review. *Nanoscale* **2022**, *14*, 16710–16730. [[CrossRef](#)] [[PubMed](#)]
14. Painter, O.; Lee, R.; Scherer, A.; Yariv, A.; O'Brien, J.; Dapkus, P.; Kim, I. Two-Dimensional Photonic Band-Gap Defect Mode Laser. *Science* **1999**, *284*, 1819–1821. [[CrossRef](#)] [[PubMed](#)]
15. Vučković, J.; Lončar, M.; Mabuchi, H.; Scherer, A. Design of photonic crystal microcavities for cavity QED. *Phys. Rev. E* **2001**, *65*, 016608. [[CrossRef](#)] [[PubMed](#)]
16. Zhen, B.; Chua, S.; Lee, J.; Rodriguez, A.; Liang, X.; Johnson, S.; Shapira, O. Enabling enhanced emission and low-threshold lasing of organic molecules using special Fano resonances of macroscopic photonic crystals. *Proc. Natl. Acad. Sci. USA* **2013**, *110*, 13711–13716. [[CrossRef](#)] [[PubMed](#)]
17. Hood, C.; Kimble, H.; Ye, J. Characterization of high-finesse mirrors: Loss, phase shifts, and mode structure in an optical cavity. *Phys. Rev. A* **2001**, *64*, 033804. [[CrossRef](#)]
18. Buck, J.; Kimble, H. Optimal sizes of dielectric microspheres for cavity QED with strong coupling. *Phys. Rev. A* **2003**, *67*, 033806. [[CrossRef](#)]
19. Hood, C.; Lynn, T.; Doherty, A.; Parkins, A.; Kimble, H. The atom-cavity microscope: Single atoms bound in orbit by single photons. *Science* **2000**, *287*, 1447–1453. [[CrossRef](#)]
20. Pinkse, P.; Fischer, T.; Maunz, P.; Rempe, G. Trapping an atom with single photons. *Nature* **2000**, *404*, 365–368. [[CrossRef](#)]

21. Rempe, G.; Thompson, R.; Kimble, H.; Lalezari, R. Measurement of ultralow losses in an optical interferometer. *Opt. Lett.* **1992**, *17*, 363–365. [[CrossRef](#)]
22. Psaltis, D.; Quake, S.; Yang, C. Developing optofluidic technology through the fusion of microfluidics and optics. *Nature* **2006**, *442*, 381–386. [[CrossRef](#)]
23. Gorodetsky, M.; Ilchenko, V. Optical microsphere resonators: Optimal coupling to high-Q whispering-gallery modes. *JOSA B* **1999**, *16*, 147–154. [[CrossRef](#)]
24. Hart, S.; Maskaly, G.; Temelkuran, B.; Prideaux, P.; Joannopoulos, J.; Fink, Y. External reflection from omnidirectional dielectric mirror fibers. *Science* **2002**, *296*, 510–513. [[CrossRef](#)] [[PubMed](#)]
25. Gorodetsky, M.; Fomin, A. Geometrical theory of whispering-gallery modes. *IEEE J. Sel. Top. Quantum Electron.* **2006**, *12*, 33–39. [[CrossRef](#)]
26. Du, W.; Zhang, S.; Shi, J.; Chen, J.; Wu, Z.; Mi, Y.; Liu, Z.; Li, Y.; Sui, X.; Wang, R.; et al. Strong exciton–photon coupling and lasing behavior in all-inorganic CsPbBr<sub>3</sub> micro/nanowire Fabry–Pérot cavity. *ACS Photonics* **2018**, *5*, 2051–2059. [[CrossRef](#)]
27. Moon, H.; Chough, Y.; Kim, J.; An, K.; Yi, J.; Lee, J. Cavity-Q-driven spectral shift in a cylindrical whispering-gallery-mode microcavity laser. *Appl. Phys. Lett.* **2000**, *76*, 3679–3681. [[CrossRef](#)]
28. Fu, L.; Lu, Q.; Liu, X.; Chen, X.; Wu, X.; Xie, S. Combining whispering gallery mode optofluidic microbubble resonator sensor with GR-5 DNAzyme for ultra-sensitive lead ion detection. *Talanta* **2020**, *213*, 120815. [[CrossRef](#)]
29. Kiraz, A.; Chen, Q.; Fan, X. Optofluidic lasers with aqueous quantum dots. *ACS Photonics* **2015**, *2*, 707–713. [[CrossRef](#)]
30. Gerard, J.; Barrier, D.; Marzin, J.; Kuszelewicz, R.; Manin, L.; Costard, E.; Rivera, T. Quantum boxes as active probes for photonic microstructures: The pillar microcavity case. *Appl. Phys. Lett.* **1996**, *69*, 449–451. [[CrossRef](#)]
31. Levy, U.; Campbell, K.; Groisman, A.; Mookherjea, S.; Fainman, Y. On-chip microfluidic tuning of an optical microring resonator. *Applied Physics Letters* **2006**, *88*, 111107. [[CrossRef](#)]
32. Armani, D.; Kippenberg, T.; Spillane, S.; Vahala, K.J. Ultra-high-Q toroid microcavity on a chip. *Nature* **2003**, *421*, 925–928. [[CrossRef](#)]
33. Li, L.; Hong, M.; Schmidt, M.; Zhong, M.; Malshe, A.; Huis, B.; Kovalenko, V. Laser nano-manufacturing—state of the art and challenges. *CIRP Ann.* **2011**, *60*, 735–755. [[CrossRef](#)]
34. Yang, L.; Armani, D.; Vahala, K. Fiber-coupled erbium microlasers on a chip. *Appl. Phys. Lett.* **2003**, *83*, 825–826. [[CrossRef](#)]
35. Wang, Y.; Leck, K.; Ta, D.; Chen, R.; Nalla, V.; Gao, Y.; Sun, H. Blue liquid lasers from solution of CdZnS/ZnS ternary alloy quantum dots with quasi-continuous pumping. *Adv. Mater.* **2015**, *27*, 169–175. [[CrossRef](#)] [[PubMed](#)]
36. Li, B.; Zhao, Y.; Zhang, Y.; Zhang, A.; Li, X.; Gu, J.; Zhou, G. Functionalized Micro Structured Optical Fibers and Devices for Sensing Applications: A Review. *J. Light. Technol.* **2021**, *39*, 3812–3823. [[CrossRef](#)]
37. Li, Z.; Psaltis, D. Optofluidic dye lasers. *Microfluid. Nanofluid.* **2008**, *4*, 145–158. [[CrossRef](#)]
38. Smart, R.; Hanna, D.; Tropper, A.; Davey, S.; Carter, S.F.; Szebesta, D. CW room temperature upconversion lasing at blue, green and red wavelengths in infrared-pumped Pr<sup>3+</sup>-doped fluoride fibre. *SPIE Milest. Ser.* **2000**, *161*, 379–381. [[CrossRef](#)]
39. Gather, M.; Yun, S. Single-cell biological lasers. *Nature Photonics* **2011**, *5*, 406–410. [[CrossRef](#)]
40. Martino, N.; Kwok, S.; Liapis, A.; Forward, S.; Jang, H.; Kim, H.; Yun, S. Wavelength-encoded laser particles for massively multiplexed cell tagging. *Nat. Photonics* **2019**, *13*, 720–727. [[CrossRef](#)]
41. Klimov, V.; Mikhailovsky, A.; Xu, S.; Malko, A.; Hollingsworth, J.; Leatherdale, A.; Bawendi, M. Optical gain and stimulated emission in nanocrystal quantum dots. *Science* **2000**, *290*, 314–317. [[CrossRef](#)]
42. Shapira, O.; Kuriki, K.; Orf, N.; Abouraddy, A.; Benoit, G.; Viens, J.; Brewster, M. Surface-emitting fiber lasers. *Opt. Express* **2006**, *14*, 3929–3935. [[CrossRef](#)] [[PubMed](#)]
43. Stolyarov, A.; Wei, L.; Shapira, O.; Sorin, F.; Chua, S.; Joannopoulos, J.; Fink, Y. Microfluidic directional emission control of an azimuthally polarized radial fibre laser. *Nat. Photonics* **2012**, *6*, 229–233. [[CrossRef](#)]
44. Zhang, M.; Liu, J.; Cheng, W.; Cheng, J.; Zheng, Z. A tunable optical Bragg grating filter based on the droplet sagging effect on a superhydrophobic nanopillar array. *Sensors* **2019**, *19*, 3324. [[CrossRef](#)]
45. Hu, J.; Fu, D.; Xia, C.; Zhang, C.; Yao, L.; Lu, C.; Liu, Y. A three-layer egg-configured Bragg microcavity of polyglycerol coated cholesteric-liquid-crystal encapsulated by hollow-glass-microsphere. *Liq. Cryst.* **2020**, *47*, 508–515. [[CrossRef](#)]
46. Helbo, B.; Kristensen, A. Menon. A micro-cavity fluidic dye laser. *J. Micromechanics Microengineering* **2003**, *13*, 307. [[CrossRef](#)]
47. Kou, Q.; Yesilyurt, I.; Chen, Y. Collinear dual-color laser emission from a microfluidic dye laser. *Appl. Phys. Lett.* **2006**, *88*, 091101. [[CrossRef](#)]
48. Aubry, G.; Kou, Q.; Soto-Velasco, J.; Wang, C.; Meance, S.; He, J.; Haghiri-Gosnet, A. A multicolor microfluidic droplet dye laser with single mode emission. *Appl. Phys. Lett.* **2011**, *98*, 111111. [[CrossRef](#)]
49. Zhou, H.; Feng, G.; Yao, K.; Yang, C.; Yi, J.; Zhou, S. Fiber-based tunable microcavity fluidic dye laser. *Opt. Lett.* **2013**, *38*, 3604–3607. [[CrossRef](#)] [[PubMed](#)]
50. Gerosa, R.; Sudirman, A.; Menezes, L.; Margulis, W.; de Matos, C. All-fiber high repetition rate microfluidic dye laser. *Optica* **2015**, *2*, 186–193. [[CrossRef](#)]
51. Kong, Y.; Dai, H.; He, X.; Zheng, Y.; Chen, X. Reconfigurable RGB dye lasers based on the laminar flow control in an optofluidic chip. *Opt. Lett.* **2018**, *43*, 4461–4464. [[CrossRef](#)] [[PubMed](#)]
52. Chen, M.; Zhao, Y.; Wei, H.; Zhu, C.; Krishnaswamy, S. 3D printed castle style Fabry–Perot microcavity on optical fiber tip as a highly sensitive humidity sensor. *Sens. Actuators B Chem.* **2021**, *328*, 128981. [[CrossRef](#)]

53. Gourley, P.; Drummond, T. Visible, room-temperature, surface-emitting laser using an epitaxial Fabry–Perot resonator with AlGaAs/AlAs quarter-wave high reflectors and AlGaAs/GaAs multiple quantum wells. *Appl. Phys. Lett.* **1987**, *50*, 1225–1227. [[CrossRef](#)]
54. Zhu, J.; Ozdemir, S.; Xiao, Y.; Li, L.; He, L.; Chen, D.R.; Yang, L. On-chip single nanoparticle detection and sizing by mode splitting in an ultrahigh-Q microresonator. *Nature photonics* **2010**, *4*, 46–49. [[CrossRef](#)]
55. Lee, W.; Sun, Y.; Li, H.; Reddy, K.; Sumetsky, M.; Fan, X. A quasi-droplet optofluidic ring resonator laser using a micro-bubble. *Appl. Phys. Lett.* **2011**, *99*, 091102. [[CrossRef](#)]
56. Sun, Y.; Suter, D.; Fan, X. Robust integrated optofluidic-ring-resonator dye lasers. *Opt. Lett.* **2009**, *34*, 1042–1044. [[CrossRef](#)]
57. Li, Z.; Zhou, W.; Liu, Y.; Ye, Q.; Ma, Y.; Wei, H.; Tian, J. Highly efficient fluorescence detection using a simplified hollow core microstructured optical fiber. *Appl. Phys. Lett.* **2013**, *102*, 011136. [[CrossRef](#)]
58. Li, Z.L.; Zhou, W.Y.; Luo, M.M.; Liu, Y.G.; Tian, J.G. Tunable optofluidic microring laser based on a tapered hollow core microstructured optical fiber. *Opt. Express* **2015**, *23*, 10413–10420. [[CrossRef](#)]
59. Gong, C.; Gong, Y.; Chen, Q.; Rao, Y.; Peng, G.; Fan, X. Reproducible fiber optofluidic laser for disposable and array applications. *Lab Chip* **2017**, *17*, 3431–3436. [[CrossRef](#)]
60. Gao, R.; Lu, D.; Zhang, M.; Qi, Z. Optofluidic immunosensor based on resonant wavelength shift of a hollow core fiber for ultratrace detection of carcinogenic benzo [a] pyrene. *ACS Photonics* **2018**, *5*, 1273–1280. [[CrossRef](#)]
61. Yu, J.; Liu, Y.; Wang, Y.; Zheng, Z.; Wang, Z.; Zhang, X.; Liu, X.; Wang, P. Optofluidic laser based on a hollow-core negative-curvature fiber. *Nanophotonics* **2018**, *7*, 1307–1315. [[CrossRef](#)]
62. Zhang, M.; Cheng, W.; Zheng, Z.; Cheng, J.; Liu, J. Meridian whispering gallery modes sensing in a sessile microdroplet on micro/nanostructured superhydrophobic chip surfaces. *Microfluid. Nanofluid.* **2019**, *23*, 1–13. [[CrossRef](#)]
63. Xu, Y.; Gong, C.; Chen, Q.; Luo, Y.; Wu, Y.; Wang, Y.; Gong, Y. Highly reproducible, isotropic optofluidic laser based on hollow optical fiber. *IEEE J. Sel. Top. Quantum Electron.* **2018**, *25*, 1–6. [[CrossRef](#)]
64. Lin, J.; Chiu, C.; Mo, T.; Lee, C. All-Optical Directional Control of Emission in a Photonic Liquid Crystal Fiber Laser. *J. Light. Technol.* **2020**, *38*, 5149–5156. [[CrossRef](#)]
65. Moon, H.; Chough, Y.; An, K. Cylindrical microcavity laser based on the evanescent-wave-coupled gain. *Phys. Rev. Lett.* **2000**, *85*, 3161. [[CrossRef](#)]
66. Li, Z.L.; Liu, Y.G.; Yan, M.; Zhou, W.Y.; Ying, C.F.; Ye, Q.; Tian, J.G. A simplified hollow-core microstructured optical fibre laser with microring resonators and strong radial emission. *Appl. Phys. Lett.* **2014**, *105*, 071902. [[CrossRef](#)]
67. Gong, C.; Gong, Y.; Zhao, X.; Luo, Y.; Chen, Q.; Tan, X.; Wu, Y.; Fan, X.; Peng, G.D.; Rao, Y.J. Distributed fibre optofluidic laser for chip-scale arrayed biochemical sensing. *Lab Chip* **2018**, *18*, 2741–2748. [[CrossRef](#)]
68. Yan, D.; Liu, B.; Zhang, H.; Zhou, W.; Ying, C.; Ye, Q.; Tian, J. Observation of lasing emission based on a hexagonal cavity embedded in a Kagome PCF. *IEEE Photonics Technol. Lett.* **2018**, *30*, 1202–1205. [[CrossRef](#)]
69. Zhao, X.; Wang, Y.; Liao, C.; Peng, G.D.; Gong, Y.; Wang, Y. Polymer-coated hollow fiber optofluidic laser for refractive index sensing. *J. Light. Technol.* **2020**, *38*, 1550–1556. [[CrossRef](#)]
70. Yoshida, Y.; Nishihara, Y.; Fujii, A.; Ozaki, M.; Yoshino, K.; Kim, H.; Choi, S. Optical properties and microring laser of conducting polymers with Sn atoms in main chains. *J. Appl. Phys.* **2004**, *95*, 4193–4196. [[CrossRef](#)]
71. Yoshida, Y.; Nishimura, T.; Fujii, A.; Ozaki, M.; Yoshino, K. Dual ring laser emission of conducting polymers in microcapillary structures. *Appl. Phys. Lett.* **2005**, *86*, 141903. [[CrossRef](#)]
72. Sun, Y.; Fan, X. Distinguishing DNA by Analog-to-Digital-like Conversion by Using Optofluidic Lasers. *Angew. Chem. Int. Ed.* **2012**, *51*, 1236–1239. [[CrossRef](#)] [[PubMed](#)]
73. Chen, Q.; Ritt, M.; Sivaramakrishnan, S.; Sun, Y.; Fan, X. Optofluidic lasers with a single molecular layer of gain. *Lab Chip* **2014**, *14*, 4590–4595. [[CrossRef](#)] [[PubMed](#)]
74. Lee, W.; Chen, Q.; Fan, X.; Yoon, D. Digital DNA detection based on a compact optofluidic laser with ultra-low sample consumption. *Lab Chip* **2016**, *16*, 4770–4776. [[CrossRef](#)] [[PubMed](#)]
75. Protesescu, L.; Yakunin, S.; Bodnarchuk, M.; Krieg, F.; Caputo, R.; Hendon, C.H.; Kovalenko, M. Nanocrystals of cesium lead halide perovskites (CsPbX<sub>3</sub>, X = Cl, Br, and I): Novel optoelectronic materials showing bright emission with wide color gamut. *Nano Lett.* **2015**, *15*, 3692–3696. [[CrossRef](#)]
76. Li, X.; Wu, Y.; Zhang, S.; Cai, B.; Gu, Y.; Song, J.; Zeng, H. CsPbX<sub>3</sub> quantum dots for lighting and displays: Room-temperature synthesis, photoluminescence superiorities, underlying origins and white light-emitting diodes. *Adv. Funct. Mater.* **2016**, *26*, 2435–2445. [[CrossRef](#)]
77. Rogacha, A. Water resistant CsPbX<sub>3</sub> nanocrystals coated by polyhedral oligomeric silsesquioxane and their use as solid state luminophores in all-perovskite white light emitting devices. *Chem. Sci.* **2016**, *7*, 5699–5703.
78. Zhang, N.; Liu, H.; Stolyarov, A.; Zhang, T.; Li, K.; Shum, P.P.; Wei, L. Azimuthally polarized radial emission from a quantum dot fiber laser. *ACS Photonics* **2016**, *3*, 2275–2279. [[CrossRef](#)]
79. Luo, M.; Liu, Y.; Wang, Z.; Li, Z.; Zhou, W.Y.; Guo, J.; Liu, X. Manipulative dual-microsphere lasing based on nanosilica waveguide integrated in a simplified hollow-core microstructured optical fiber. *J. Light. Technol.* **2017**, *35*, 2183–2189. [[CrossRef](#)]
80. Shi, H.; He, J.; Guo, H.; Liu, X.; Wang, Z.; Liu, Y. Single-resonator, stable dual-longitudinal-mode optofluidic microcavity laser based on a hollow-core microstructured optical fiber. *Opt. Express* **2021**, *29*, 10077–10088. [[CrossRef](#)]

81. Yu, J.; Liu, Y.; Luo, M.; Wang, Z.; Yang, G.; Zhang, H.; Zhang, X. Single longitudinal mode optofluidic microring laser based on a hollow-core microstructured optical fiber. *IEEE Photonics J.* **2017**, *9*, 1–10. [[CrossRef](#)]
82. Shi, H.; Yu, J.; Guo, H.; Wang, Z.; Liu, X.; Liu, Y. Fluid-controlled stable single longitudinal mode microcavity laser based on an antiresonant hollow-core fiber. *Laser Phys. Lett.* **2020**, *17*, 025101. [[CrossRef](#)]

**Disclaimer/Publisher’s Note:** The statements, opinions and data contained in all publications are solely those of the individual author(s) and contributor(s) and not of MDPI and/or the editor(s). MDPI and/or the editor(s) disclaim responsibility for any injury to people or property resulting from any ideas, methods, instructions or products referred to in the content.